

Comparison of Voltage Stability Indices Based on Synchronized PMU Measurements

Valéria Monteiro de Souza
Department of Electric Energy
NTNU
Trondheim, Norway
valeria.m.de.souza@ntnu.no

Hugo Rodrigues de Brito
Department of Electric Energy
NTNU
Trondheim, Norway
hugo.r.de.brito@ntnu.no

Kjetil Obstfelder Uhlen
Department of Electric Energy
NTNU
Trondheim, Norway
kjetil.uhlen@ntnu.no

Abstract—The need for reliable information about the status of electrical power systems is an increasingly relevant concern within the current trend of electrification and deployment of power electronics-based devices. In this scenario, methods of real-time monitoring of power system long-term voltage stability using synchronized phasor measurements play an important role. This paper conducts the assessment and comparison of three well-established approaches to this issue, based solely on local measurements, in terms of different types of loads, line disconnection events, placement of monitoring devices and presence of noise in the synchronized measurements. The comparative analyses are derived from dynamic simulation data of a 3-bus test system as well as of the IEEE 9-bus network, both modelled in the open-source Python-based power system simulator DynPSSimPy. Results focus on the robustness and accuracy of each method in detecting the point of maximum power transfer, showing their advantages and drawbacks under different system conditions.

Index Terms—Voltage stability, synchrophasors, dynamic simulation, real-time monitoring, maximum power transfer.

I. INTRODUCTION

A. Motivation and Background

Electrical power grids throughout the world have been changing significantly with the increasing penetration of power electronics-interfaced technologies, such as wind power and photovoltaic generation. This scenario, combined with the progressive increase in load demand and lack of necessary transmission grid reinforcements, leads to challenges to the proper operation and control of power systems in a robust, reliable and efficient way. In recent years, these developments have reinforced the need to update definitions of previously well-known stability phenomena, with the introduction of two new categories of stability: resonance and converter-driven [1].

Risks associated to insufficient stability margins are substantial (rise of incidents such as system splits, cascading faults, equipment damage, blackouts, etc.), and the changing nature of electrical power grid characteristics is prone to making stability issues become as common and as important as congestion management is today. Therefore, research and development of new technological contributions towards stable grid operation, such as advanced monitoring and control, are a key demand of system operators [2], [3].

A particularly relevant feature is the transmission system's load supply capabilities as a means to avoid voltage instability issues - considered by many as the biggest threat to power system operation. In this context, a real-time voltage stability index (VSI) that accurately pinpoints voltage stability margins and allows for sufficiently fast triggering of corrective measures whenever applicable, with the end goal of enhancing network reliability, is a desirable asset to the ongoing trend of modernization of grid control centers [4].

B. Relevant Literature

Literature related to this research topic is extensive, and several approaches have been proposed to the development of VSIs suitable for real-time monitoring [5]. Many of these VSIs are inspired by the use of synchronized Phasor Measurement Units (PMUs), due to their high sampling rate and pervasiveness throughout electrical power systems worldwide [6], [7]. Some of these methods rely solely on PMU data [8]–[10], whereas others require additional network topology information [11]–[13].

In [14], a VSI that identifies Thévenin voltage and impedance equivalents from local PMU measurements of an extra high voltage bus was presented. A large Italian power system was modelled and used to evaluate sensitivity, reliability, robustness and effectiveness of the proposed algorithm.

In [15], a VSI that works with variations of the apparent power and impedance given by PMU measurements was presented. The algorithm is applicable to transmission and sub-transmission systems, and was validated through simulations of a 130 kV subsystem in Northern Norway with real PMU data from the Nordic power grid.

In [16], local PMU measurements were used to calculate changes in active power and in the apparent conductance seen by the target bus, resulting in a novel VSI formulation suited for both radial and meshed systems. The IEEE Nordic Test System was the benchmark chosen to validate the algorithm in terms of dependability and security.

C. Contributions and Organization

The present paper highlights the most significant advantages and disadvantages of each method. Furthermore, a contribution is made towards the ongoing discussion on how the placement

of monitoring devices impacts the accuracy of different VSIs. The paper is organized as follows: Section II provides an overview of the theoretical background of the three aforementioned VSIs; Section III describes the methodology adopted for the dynamic simulations of both a 3-bus test system and the IEEE 9-bus network; Section IV presents the results of the performance assessment, which covers sensitivity analyses related to different load types, line disconnection events and presence of measurement noise; and Section V concludes the paper.

II. VOLTAGE STABILITY INDICES BASED ON PMU MEASUREMENTS

A. Adaptive Method (AD)

The Adaptive Method (AD) is a VSI based on the Thévenin equivalent presented in [14]. This VSI is suited for high voltage transmission-level buses, where it is possible to assume that the Thévenin resistance is negligible ($R_{th} \approx 0$). The main equations used in this algorithm are:

$$\beta = \arccos\left(\frac{V_L \cos \theta}{E_{th}}\right) \quad (1)$$

$$X_{th} = \frac{E_{th} \sin \beta - V_L \sin \theta}{I_L} \quad (2)$$

where V_L is the load voltage magnitude, I_L is the load current magnitude, θ is the angle between load voltage and load current, E_{th} is the Thévenin voltage magnitude, β is the angle between Thévenin voltage and load current and X_{th} is the Thévenin reactance. The first three variables are known from PMU measurements, whereas the last three are unknown.

The idea behind this method is to set E_{th} as a free variable and iteratively guess its value for every new available PMU measurement. Increments or decrements are made depending on whether the previous guess is under or over-estimated, respectively, in order to direct E_{th} towards its real value. The initial guess and iterative variation of E_{th} are given respectively by:

$$E_{th0} = \frac{1}{2}(E_{th_{max}} + E_{th_{min}}) = \frac{1}{2}\left(\frac{V_L \cos \theta}{\cos \beta_{max}} + V_L\right) \quad (3)$$

$$\varepsilon_E = \min\left(\left|E_{th}^{i-1} - V_L^i\right|, \left|E_{th}^{i-1} - E_{th}^{max(i)}\right|, \left|E_{th}^{i-1} k\right|\right) \quad (4)$$

where $E_{th_{min}}$ is the minimum value of E_{th} , $E_{th_{max}}$ is the maximum value of E_{th} , $\beta_{max} = \arctan((1 + \sin \theta)/\cos \theta)$, i is the corresponding time step, and k is a pre-specified parameter that usually ranges from 0.0001 to 0.001.

After estimating E_{th0} from (3), E_{th} is updated according to the variations of load impedance (ΔZ_L) and Thévenin reactance (ΔX_{th}) as follows:

- If ΔZ_L and ΔX_{th} have the same sign, E_{th}^i is to be increased by ε_E .
- If ΔZ_L and ΔX_{th} have opposite signs, E_{th}^i is to be decreased by ε_E .

- If $\Delta X_{th} = 0$, convergence is achieved.

With the updated value of E_{th} , β can be calculated from (1) and X_{th} from (2). If the correct value of E_{th} is achieved, then β and X_{th} will have reached their correct value as well.

The VSI itself can thus be defined as in (5), so that the point of maximum power transfer happens when $X_{th} = Z_L$.

$$AD = \frac{X_{th}}{Z_L} \quad (5)$$

B. S-Z sensitivity indicator (SZI)

The VSI named S-Z sensitivity indicator (SZI), proposed in [15], can be defined as:

$$SZI = \frac{\Delta S}{\Delta Z} \quad (6)$$

where ΔS and ΔZ represent, respectively, the difference between two consecutive measurements of apparent power and impedance as seen by the PMU device.

For this VSI, a negative value during a load increase scenario ($\Delta Z < 0$) means that the system is providing the required load demand ($\Delta S > 0$) and maximum power transfer has not been reached. On the other hand, a positive SZI value during a load increase scenario means that the system is not meeting the load demand ($\Delta S < 0$) and maximum power transfer has been reached. Therefore, the point of maximum power transfer happens when SZI is equal to zero.

Since this index is based on differences (ΔS and ΔZ), certain considerations have to be made so as to prevent false alarms that might arise from random variations, measurement noise, short-term dynamics, etc. First, only two consecutive measurements that result in a negative and sufficiently large ΔZ are considered. By doing so, the impact of noise in the PMU measurement is mitigated, and the SZI output focuses only on load increase scenarios, which are the most critical from a voltage stability standpoint. Moreover, after computing the SZI from ΔS and ΔZ , a moving average filter must be applied to provide the final index.

In order to facilitate the comparative analysis with the other VSIs assessed in this paper, the preferred definition for SZI is as given in (7). With this adjustment, maximum power transfer occurs instead when the index reaches the unit value.

$$SZI = 1 + \frac{\Delta S}{\Delta Z} \quad (7)$$

An interesting feature of the SZI which is outside the scope of this paper is that it can also be used to estimate Thévenin parameters of the system.

C. New Local Identification of Voltage Emergency Situations Index (NLI)

The VSI named New Local Identification of Voltage Emergency Situations Index (NLI) presented in [16] can be defined as:

$$NLI = \frac{\Delta P}{\Delta G} \quad (8)$$

where ΔP and ΔG represent, respectively, the difference between two consecutive measurements of active power and conductance as seen by the PMU device.

The main concept of this method is that, for a continuous increase in conductance, the NLI remains positive up to the maximum power transfer condition and becomes negative past this point. This occurs because ΔG remains positive whereas ΔP becomes negative after reaching maximum power transfer.

An important aspect of this VSI is that, since it relies on differences (ΔP and ΔG), a proper filtering technique needs to be applied in order to mitigate the influence of measurement noise and short-term dynamics in the index results. Additionally, an even better NLI performance can be attained by disregarding measurements that provide negative or negligible values of ΔG . The filtering approach employed in this paper consists of several layers of moving average calculations.

A slight modification in the NLI definition, similar to what was done in the SZI case, is made in this paper as a means to facilitate the comparative analysis. This is shown in (9), indicating that the point of maximum power transfer occurs instead when the index reaches the unit value.

$$NLI = 1 - \frac{\Delta P}{\Delta G} \quad (9)$$

III. METHODOLOGY

Performance assessment and comparisons of the three VSIs were based on data from dynamic simulations carried out in the open-source Python-based power system simulator DynPSSimPy [17]. All simulations had a sampling rate of 50 Hz, i.e., voltage and current phasors required for the VSI algorithms were acquired every 20 ms just as is done via PMUs. Loads within the test systems were increased throughout the analyses so as to reproduce conditions conducive to voltage instability scenarios.

A. Simple 3-Bus test system

A simple 3-bus test system, illustrated in Fig. 1, was used to investigate how the placement of monitoring devices impacts the accuracy of VSIs. To this end, voltage and current phasor measurements were obtained from buses $B2$ and $B3$. The load was modelled as constant impedance, with a constant power factor of 0.98, and varied over time as shown in Fig. 2.

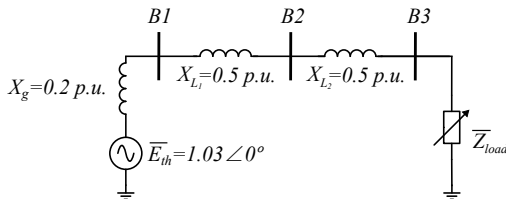


Fig. 1. Single-line diagram of the 3-bus test system.

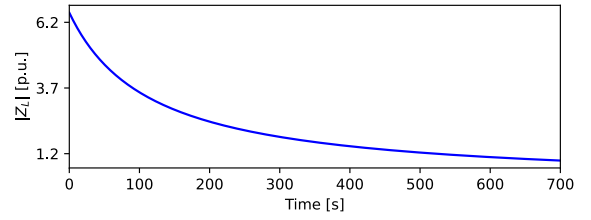


Fig. 2. Variation over time of load impedance magnitude.

B. IEEE 9-bus network

The IEEE 9-bus network (Fig. 3) was used to conduct the impact assessment of different load types: constant power, constant current, constant impedance and ZIP model. The loads in buses $B5$, $B6$ and $B8$ were increased relative to their base values in a rate of 0.1%/s, 0.2%/s and 0.3%/s respectively.

Furthermore, performance evaluations of the VSIs were conducted in three scenarios: disconnection of Line 4-5 (located between buses $B4$ and $B5$), disconnection of Line 8-9 (located between buses $B8$ and $B9$) and presence of Gaussian noise in phasor measurements. The ZIP load model was adopted in all three cases, and line disconnection events were set to take place after 70 seconds of simulation.

The latter of the three scenarios refers to the addition of Gaussian noise with standard deviation of $\sigma = 0.01/3$ and mean value $\mu = 0$ to both magnitude and phase of current and voltage measurements, which is described in [16] as a worst-case scenario.

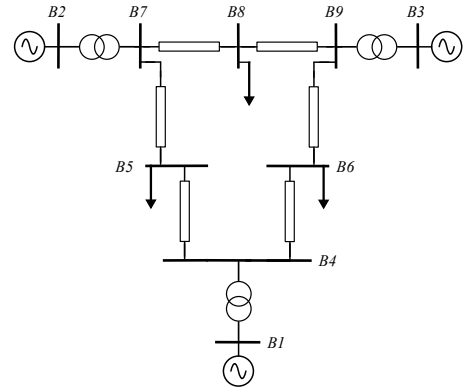


Fig. 3. Single-line diagram of the IEEE 9-bus network.

IV. RESULTS

Dynamic simulation results are presented in this section, accompanied by a discussion on the accuracy of each of the three methods in identifying the point of maximum power transfer (PMPT). In order to facilitate its visualization, figures also include the PMPT as a black dot and a subplot focused on the VSI profiles in the vicinity of this point. Furthermore, a black dashed line was added to the plots to better indicate the moment when each VSI reaches the unit value, as per equations (5), (7) and (9).

A. Placement of monitoring device

Fig. 4 shows the VSIs for the case where measurements are taken from the test system in Fig. 1, exactly at the load bus B3. The AD and SZI methods are able to identify the PMPT roughly at the same time, with almost no delay when compared to the actual PMPT. The NLI method, on the other hand, has a delay of around 4 seconds in detecting the PMPT, which can be explained by the extra filtering steps needed in this method. It is worth mentioning that all VSIs require a certain amount of initialization time to stabilize.

It is evident that the SZI method behavior differs widely from the other two VSIs. This happens because, in this VSI, the overall closeness to the unit value is not as meaningful as the general indicator movement towards this value and the speed in which this trajectory is delineated. This illustrates that small differences in VSI formulation lead to different interpretations of output data.

Fig. 5 shows the VSI responses with the point of measurement changed to bus B2. In this scenario, the NLI is the only method capable of identifying that the PMPT has been reached within the chosen simulation time window. The detection delay is approximately the same as in the previous case, which attests to the indicator's robustness to PMU placement.

Between the two remaining indicators, the AD is clearly less accurate. This is a direct consequence of the method's necessary condition for accuracy: measurements have to be obtained from a constant power factor bus [16]. The same logic applies to a lesser extent to the SZI method, since it depends on apparent power iterative variations.

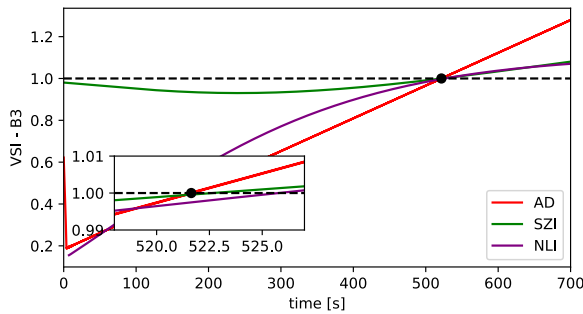


Fig. 4. VSIs - B3 bus as the place of monitoring.

B. Different types of load

Results within this subsection are derived from the test system of Fig. 3, and are intended to assess VSI performance under different load models: constant power (Fig. 6), constant current (Fig. 7), constant impedance (Fig. 8) and ZIP (Fig. 9). In this network, the load increasing results in the restriction of generators' field voltage by their respective automatic voltage regulators, starting between 300s and 400s of simulation and ultimately leading the system towards instability.

Among all scenarios, smaller VSI errors in identifying the PMPT are achieved with constant power loads, as Fig. 6 indicates. In this case, the NLI method presents the biggest

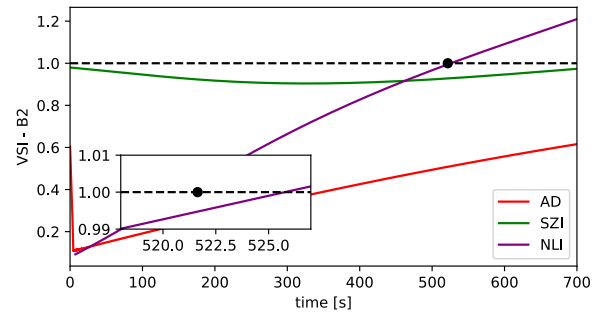


Fig. 5. VSIs - B2 bus as the place of monitoring.

delay at around 1.26 seconds, whereas the AD method presents the lowest delay at around 0.75 seconds.

For constant current loads, Fig. 7 shows that the maximum VSI delay of approximately 4 seconds comes from the NLI method, whereas the AD and SZI methods fare much better with delays of less than 1 second.

The worst-case scenario arises from modelling the loads as constant impedances, as shown in Fig. 8. This happens because the non-linearity of system equations as the load model becomes more voltage-dependent tends to worsen PMPT detection by the VSIs. Nevertheless, the SZI method is robust enough to postpone PMPT detection by only 1 second. As in the constant current case, the NLI method is able to maintain its delay in the region of 4 seconds. Conversely, the AD indicator presents a severe delay of 23 seconds in identifying the PMPT, which constitutes a clear performance limitation of the adaptive method.

Lastly, Fig. 9 shows VSI responses to a ZIP load model. The hybrid nature of ZIP parameters makes it so that overall VSI behavior is very similar to the constant current case, average individual delays included.

It is worth noticing that both the SZI and NLI methods produce consistent results regardless of the load model, with the SZI being the most accurate indicator overall. On the other hand, the AD method increasingly struggles to detect the PMPT as loads get more voltage-dependent, responding particularly poorly to the constant impedance model.

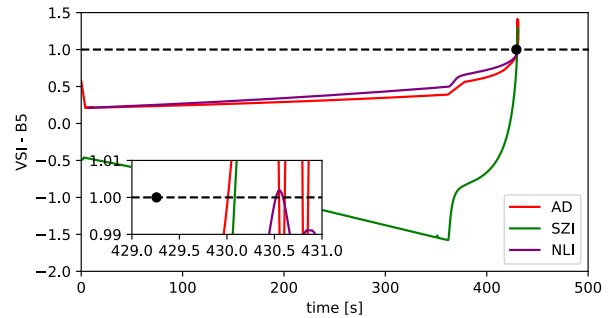


Fig. 6. VSIs - System with constant power loads.

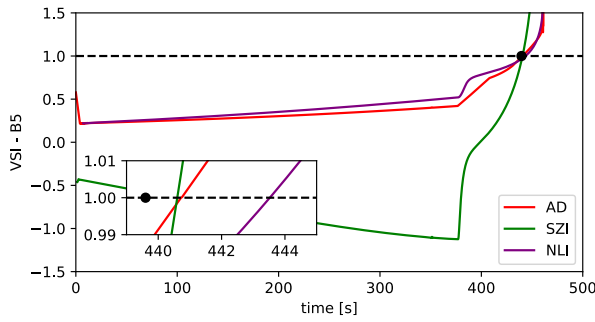


Fig. 7. VSIs - System with constant current loads.

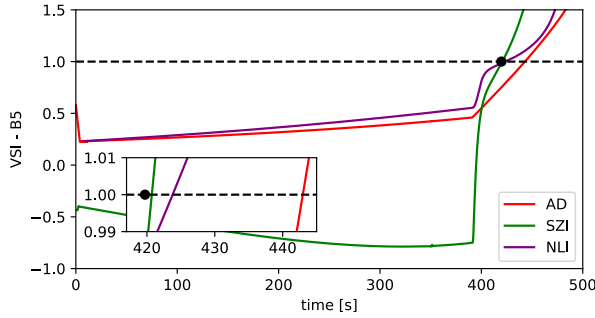


Fig. 8. VSIs - System with constant impedance loads.

C. Line disconnection events

Results for the line disconnection events carried out in the 9-bus network are shown in Fig. 10 and Fig. 11. It can be observed that all indicators go through a transient period immediately after the disconnection events at $t = 70$ seconds, lasting around 15 seconds in total. This time span for adaptation to the reconfigured system is unavoidable, since all VSI formulations iteratively depend on past measurements. However, the impact on each method's behavior is different: whereas the AD trajectory only changes slightly, the NLI and SZI methods present significant spike responses, which raise the concern of triggering false alarms.

Fig. 10 shows that, when the line closest to the monitored bus is disconnected, both indicators surpass the unit value

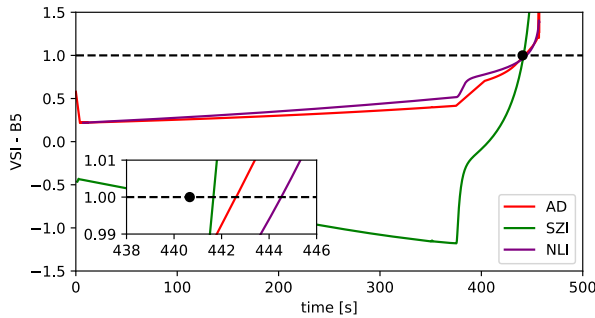


Fig. 9. VSIs - System with ZIP loads.

threshold, thereby prompting a false alarm of voltage instability. The situation is less severe in Fig. 11, where disconnection of a line distant from the point of monitoring leads to a false alarm via the SZI method, but not via the NLI method (albeit by quite a small margin). The results from these VSIs could be improved by increasing the number of samples of their moving averages. However, considering the potential delay in detecting the PMPT due to increased dependence on previous measurements, a cost-benefit analysis is recommended.

Regarding PMPT detection, the SZI and NLI methods remain consistent in both cases in terms of time delays, with the SZI being the most accurate overall. Conversely, the AD method responds much better to the disconnection of Line 4-5 than of Line 8-9, meaning that proximity to the point of monitoring markedly affects its accuracy for this network.

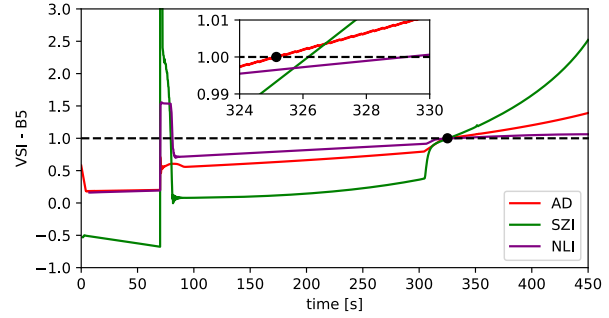


Fig. 10. VSIs - Disconnection of Line 4-5.

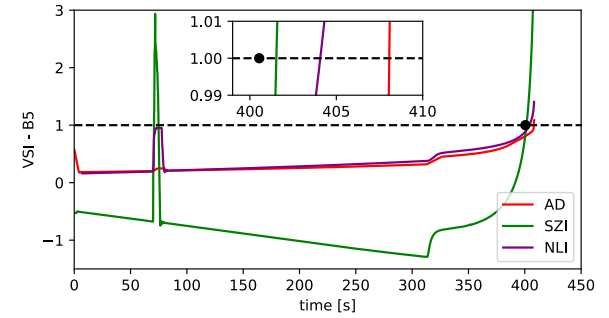


Fig. 11. VSIs - Disconnection of Line 8-9.

D. Presence of noise in the measurements

Fig. 12 shows VSI performance for the scenario of Gaussian noise in the measurements. When compared to previous studies of the 9-bus network, it is noticeable that the presence of noise significantly affects the performance of all indicators.

VSI responses vary widely in terms of trajectory and PMPT detection: the AD method presents the cleanest trend among the VSIs studied due to its inherent filtering characteristic [18], but it underestimates the PMPT by more than 100 seconds; the NLI method is also able to handle the added error, but it identifies the PMPT with around 11 seconds of delay; the SZI method, however, is not suited for this application as it triggers

several consecutive false alarms. For the latter, it is evident that a better adjustment of the employed moving average, or the inclusion of extra filtering steps along the iterative process, would greatly benefit its robustness to measurement noise.

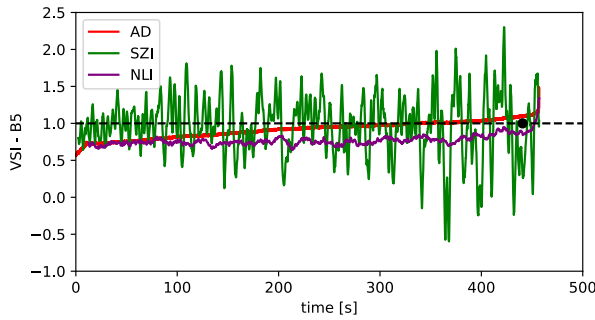


Fig. 12. VSIs - Measurements with added Gaussian noise.

V. CONCLUSION

This paper provided a performance assessment and comparative analysis of three on-line VSIs based solely on synchronized phasor measurements. Different system conditions were addressed within the discussion of each indicator's robustness and accuracy in detecting the PMPT.

The Thévenin-based AD method has a straightforward accuracy condition, which makes it ideally suited for load bus monitoring, constant power load modelling and line disconnection events. However, it gets progressively less accurate if the power factor is not constant at the point of monitoring, and as load models become more voltage-dependent. It might also lead to conservative PMPT estimations in the presence of measurement noise.

The sensitivity-based SZI method is remarkably effective in dealing with different load models, especially as they get more voltage-dependent. Its main drawback relates to its tendency of triggering false alarms both during line disconnection events and, to a much larger extent, when noise is involved. Further work on filtering adjustments is expected to improve the indicator's robustness in this regard.

Finally, the sensitivity-based NLI method presents the best results for different points of monitoring and for the scenario involving Gaussian noise. The main concern regarding this method is also its tendency of triggering false alarms during line disconnection events.

It is clear that, for the VSIs to be used in control center applications to provide alarms of voltage instability events, a threshold lower than one needs to be defined considering the system dynamics, response time of corrective actions, and the desired level of grid security.

Future work aims to expand the scope of the comparative study, including the influence of on-load tap changers, over-excitation limiters and power electronics-based devices on VSI accuracy. Furthermore, special focus will be placed on the Nordic power grid, through analyses derived from real data

for past voltage instability events that will provide valuable insights for determining the appropriate threshold for this grid.

ACKNOWLEDGMENT

We gratefully acknowledge the support from The Research Council of Norway and industry partners through Research Council project "ref: 309326" (NEWEPS).

REFERENCES

- [1] N. Hatzargyriou *et al.*, "Definition and Classification of Power System Stability – Revisited & Extended," *IEEE Transactions on Power Systems*, vol. 36, no. 4, pp. 3271–3281, Jul. 2021.
- [2] ENTSO-E, "Stability Management in Power Electronics Dominated Systems." [Online]. Available: <https://www.entsoe.eu/news/2022/06/21/entso-e-publishes-a-position-paper-on-stability-management-in-power-electronics-dominated-systems/>
- [3] ENTSO-E, "A Power System for a Carbon Neutral Europe." [Online]. Available: <https://www.entsoe.eu/news/2022/10/11/entso-e-vision-a-power-system-for-a-carbon-neutral-europe/>
- [4] T. Van Cutsem *et al.*, "Test Systems for Voltage Stability Studies," *IEEE Transactions on Power Systems*, vol. 35, no. 5, pp. 4078–4087, Sep. 2020.
- [5] M. Glavic and T. Van Cutsem, "A short survey of methods for voltage instability detection," in *2011 IEEE Power and Energy Society General Meeting*, Jul. 2011, pp. 1–8.
- [6] F. Aminifar, M. Fotuhi-Firuzabad, A. Safdarian, A. Davoudi, and M. Shahidehpour, "Synchrophasor Measurement Technology in Power Systems: Panorama and State-of-the-Art," *IEEE Access*, vol. 2, pp. 1607–1628, 2014.
- [7] A. Vaccaro and A. Zobaa, Eds., *Wide area monitoring, protection and control systems: the enabler for smarter grids*. IET Digital Library, Aug. 2016. [Online]. Available: <https://digital-library.theiet.org/content/books/po/pbpo073e>
- [8] B. Milosevic and M. Begovic, "Voltage-stability protection and control using a wide-area network of phasor measurements," *IEEE Transactions on Power Systems*, vol. 18, no. 1, pp. 121–127, Feb. 2003.
- [9] F. Hu, K. Sun, A. Del Rosso, E. Farantatos, and N. Bhatt, "Measurement-Based Real-Time Voltage Stability Monitoring for Load Areas," *IEEE Transactions on Power Systems*, vol. 31, no. 4, pp. 2787–2798, Jul. 2016.
- [10] C. Liu *et al.*, "Measurement-Based Voltage Stability Assessment Considering Generator VAR Limits," *IEEE Transactions on Smart Grid*, vol. 11, no. 1, pp. 301–311, Jan. 2020.
- [11] Y. Wang *et al.*, "Voltage Stability Monitoring Based on the Concept of Coupled Single-Port Circuit," *IEEE Transactions on Power Systems*, vol. 26, no. 4, pp. 2154–2163, Nov. 2011.
- [12] J.-H. Liu and C.-C. Chu, "Wide-Area Measurement-Based Voltage Stability Indicators by Modified Coupled Single-Port Models," *IEEE Transactions on Power Systems*, vol. 29, no. 2, pp. 756–764, Mar. 2014.
- [13] W. Xu, I. R. Pordanjani, Y. Wang, and E. Vaahedi, "A Network Decoupling Transform for Phasor Data Based Voltage Stability Analysis and Monitoring," *IEEE Transactions on Smart Grid*, vol. 3, no. 1, pp. 261–270, Mar. 2012.
- [14] S. Corsi and G. N. Taranto, "A Real-Time Voltage Instability Identification Algorithm Based on Local Phasor Measurements," *IEEE Transactions on Power Systems*, vol. 23, no. 3, pp. 1271–1279, Aug. 2008.
- [15] D. T. Duong, "Online Voltage Stability Monitoring and Coordinated Secondary Voltage Control," Doctoral thesis, NTNU, 2016. [Online]. Available: <https://ntnuopen.ntnu.no/ntnu-xmlui/handle/11250/2410911>
- [16] C. D. Vournas, C. Lambrou, and P. Mandoulidis, "Voltage Stability Monitoring From a Transmission Bus PMU," *IEEE Transactions on Power Systems*, vol. 32, no. 4, pp. 3266–3274, Jul. 2017.
- [17] H. Haugdal, K. Uhlen, and H. Jóhannsson, "An Open Source Power System Simulator in Python for Efficient Prototyping of WAMPAC Applications," in *2021 IEEE Madrid PowerTech*, Jun. 2021, pp. 1–6.
- [18] G. N. Taranto, C. Oyarce, and S. Corsi, "Further investigations on a phasor measurement-based algorithm utilized for voltage instability awareness," in *2013 IREP Symposium Bulk Power System Dynamics and Control*, Aug. 2013, pp. 1–8.